# Journal of Materials Chemistry B

Accepted Manuscript






ROYAL SOCIETY OF CHEMISTRY

www.rsc.org/materialsB

Journal Name

RSCPublishing

ARTICLE

# Water-soluble nano-fluorogens fabricated by self-assembly of bolaamphiphiles bearing AIE moieties: towards the application in cell imaging

Cite this: DOI: 10.1039/x0xx00000x

Received 00th January 2012,
Accepted 00th January 2012

DOI: 10.1039/x0xx00000x

www.rsc.org/

Yijun Xia,[a] Lin Dong,[b] Yingzhi Jin,[a] Shuai Wang,[a] Li Yan,[a] Shouchun Yin,*[b] Shixin Zhou,*[c] Bo Song*[a]

Nano-fluorogens with mono-molecule layered structure are fabricated by self-assembly of a new bolaamphiphile bearing tetraphenylethene moiety. The nano-fluorogens show good water-solubility, biocompatibility, and strong emission with a quantum yield as high as 15%. The nano-fluorogens as prepared are successfully applied to label and map the HeLa cells. The images obtained have high contrast and resolution, showing a promising potential in the line of fluorescence detecting in bio-related systems.

## Introduction

Recently fluorescence detecting, such as bio-sensing and bio-imaging,[1-7] developed rapidly and attracted a great deal of research attention, due to the requirement in the health care of human beings. Exploring the fluorogens that are suitable for those applications is the key issue. To date the fluorogens available basically have three categories: Green fluorescent protein (GFP),[8] inorganic quantum dots (e.g., CdSe, ZnS, and CdS)[9, 10] and organic molecules with conjugated aromatics.[11, 12] When using GFP as a reporter of expression for morphological differentiation, the bio-sensing process is rather complicated and time-consuming, and the unexpected morphologies can happen to the target cells.[13, 14] The quantum dots show very good emission properties, but the inherent cytotoxicity will limit its applications in bio-related areas.[15] Thus, the organic materials, owing to the large variety and easy processing feature, become high-prestige candidates as fluorogens in bio-related detecting.

In general, due to the poor miscibility, the organic aromatics are ready to aggregate at high concentrations or in the unfavorable dispersing mediums. The aggregation of molecules will usually influence the emission properties of the fluorogens.[16] For the conventional organic aromatics,[17] the emission will be quenched upon the aggregation, which decreases the sensitivity of this methodology. On the contrary, for a type of novel molecules reported by Tang's group,[18-21] as well as other groups,[22-27] the emission will be enhanced by the aggregation. This phenomenon is called aggregation induced emission (AIE).

The molecules with AIE effect have some unique advantages as being used in the bio-systems. First, the emission will not be quenched, but enhanced owing to the aggregation when being introduced into the bio-system, and thus facilitate the detection.[3, 28] Second, the emission difference at different aggregation state can be utilized as a measure for the morphological change of the proteins.[29] Third, by alternating the outer groups of the aggregates, the fluorogens can be adaptable to the targets, and have low cytotoxicity to cells and specific bonding to certain biomolecules.[30, 31]

Increasing the water-solubility and biocompatibility of the aggregates of AIE dyes are vitally important for application in bio-systems.[32] Tang et al. have designed AIE molecules as soluble salts to combine with DNAs[33] and proteins,[29] and used the emission to differentiate the conformation of the biomolecules. To improve photobleaching resistance and stability of AIE dots, AIE fluorogens which spontaneously aggregate in aqueous media have been developed by the same group.[8] Besides, fluorescent silica dots[30, 34-37] have been fabricated by incorporating AIE fluorogens into silica networks. Wei's group, as well as other groups, has separately reported the induced fluorescence enhancement of dye molecules by encapsulating with different micelles.[38-42] Developing a simple method to fabricate water-soluble, biocompatible, and low cytotoxic aggregates with AIE dyes will facilitate the application of such kind of fluorogens in bio-related systems. [43]

The ionic bolaamphiphiles with a rigid core in the middle of the molecules showed great potential for preparing stable nanostructures by self-assembly.[44-51] It played an important and irreplaceable role in the grand and long-standing research of biomimetic and bio-inspired materials.[52-61] We hypothesize that the marriage of AIE effect and bolaamphiphiles will lead to stable nano-fluorogens with certain morphology, good water-solubility and bio-compatibility.

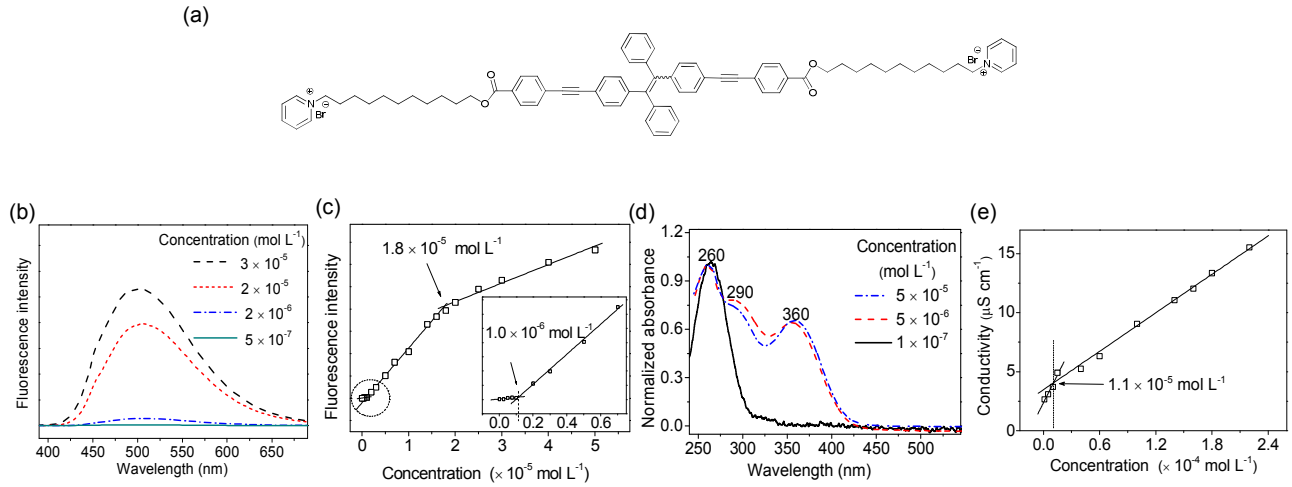


**Fig. 1** (a) Molecular structure of TPE-11. (b) Typical fluorescence spectra of TPE-11 in aqueous solution at different concentrations; (c) plot of fluorescence intensity vs. concentration of TPE-11 solution, and the inset is magnification of (c) in the vicinity of $1 \times 10^{-6}$ mol $L^{-1}$. All the fluorescence spectra are excited at 360 nm. (d) Absorption spectra of TPE-11 in aqueous solutions with concentration of $1 \times 10^{-7}$ mol $L^{-1}$, $5 \times 10^{-6}$ mol $L^{-1}$ and $5 \times 10^{-5}$ mol $L^{-1}$; (e) Concentration dependent conductivity of TPE-11 in aqueous solution.

In this work, we synthesized a bolaamphiphile with a tetraphenylethene (TPE) unit attached with two pyridinium salt-terminated alkyl groups (noted as TPE-11, Fig. 1a), and investigated its self-assembly behavior. It was found that this molecule formed mono-molecule layered nanostructures, which showed strong emission, and were successfully applied to label and map the HeLa cells by fluorescence.

## Results and discussion

Since the emission properties of TPE are correlated to its aggregation state, the fluorescence spectra were employed to investigate the self-assembly behaviour of TPE-11 in aqueous solution (Fig. 1b). When plotting the fluorescence intensity at 500 nm versus the corresponding concentration (Fig. 1c), two inflections are indicated: one locates at $1.0 \times 10^{-6}$ mol $L^{-1}$, and the other at $1.8 \times 10^{-5}$ mol $L^{-1}$ (inset of Fig. 1c). According to the experiences, the inflections suggest the change of the aggregation state. The lower inflection point should correspond to the critical micelle concentration (CMC). Above this point, the fluorescence increases dramatically, which shows a typical AIE property of TPE-11, and also serves as an indicator of the aggregation. The higher inflection can be attributed to the morphological transition of the aggregates. For convenience of description, the second inflection is noted as critical transition concentration (CTC). These two inflection points are further confirmed by the UV-vis spectra and conductivity.

As the concentration is lower than the CMC, the absorption spectrum shows a single peak at around 260 nm (Fig. 1d). Since the aggregates are not formed yet before the CMC, the absorption should correspond to the monomers. However, when the concentration is between CMC and CTC, besides the peak at around 260 nm, two new peaks appear at around 290 and 360 nm, which should be attributed to the formation of the aggregates in the solution. The data are in accordance with that indicated by the fluorescence results. Further increase of the concentration did not cause significant peak shift in the normalized absorption spectrum, as shown in Fig. 1d. The combination of absorption and fluorescence spectra gives a sound explanation about the mechanisms of AIE effect. The absorption peak at 260 nm is very close to the absorption of phenyl groups, which has been claimed previously by Tang et al.[62] The absence of the other two peaks located at around 290 and 360 nm indicates that the TPE group is not well conjugated. Without restriction of motions of phenyl ring, the absorbed energy is possibly consumed by the rotation of the phenyl groups linked to the vinyl group rather than fluorescence emission. Above the CMC, the aggregation limits the rotation of the phenyl groups due to the steric hindrance, thus leading to the large conjugated structure (i.e. the bathochromic shift of absorption), as well as the strong fluorescence.

The CTC is further confirmed by conductivity method. As shown in plot of concentration dependent conductivity in Fig. 1e, there is an inflection at $1.1 \times 10^{-5}$ mol $L^{-1}$, which is comparable with the CTC indicated by the fluorescence results. Due to the sensitivity limitation, the CMC is not detectable by this method.

Now that the self-assembly behavior has been unraveled, the most concern will be the morphology of the assemblies at different concentrations. Herein, in situ atomic force microscope (AFM) was employed to observe the adsorbed structures at the solid / liquid interface. Since the scanning is done in solution state, the images should reflect the morphologies of the assemblies without damage due to the dewetting effect. Additionally, the peak force quantitative nanomechanical mapping (QNM) in fluid method was applied to control the forces exerted on the tip as small as possible, in case of causing deformation of the assemblies. As shown by the AFM images in Fig. 2, when the concentration is between CMC and CTC, as shown in Fig. 2a (concentration = $5 \times 10^{-6}$ mol $L^{-1}$), TPE-11 mainly forms flake-like aggregates with an average diameter of 40 ± 11 nm. When the concentration is higher than the CTC, the flake-like structures are mostly elongated to hundreds of nanometers, as shown in Fig. 2b (concentration = $1 \times 10^{-3}$ mol $L^{-1}$). Although both two kinds of nanostructures were observed below and above the CTC, the population ratios of them are different. At higher concentration, the elongated structures are relative more.

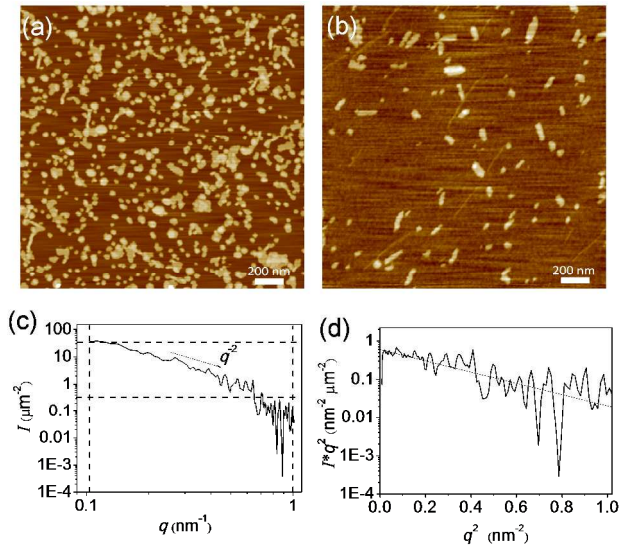


**Fig. 2** In situ AFM images of the aggregates formed at concentrations of (a) 5 × $10^{-6}$ mol $L^{-1}$ and at (b) 1 × $10^{-3}$ mol $L^{-1}$. (c) Dismeared SAXS data of TPE-11 with concentration of 5 × $10^{-3}$ mol $L^{-1}$; (d) guinier analysis of (c).

Small angle X-ray scattering (SAXS) is quite a useful tool to determine the morphology of the nanostructures in solution.[63] Therefore, it was used to prove that the assemblies are formed in the solution, but not induced by the substrate as being adsorbed on the surface. To acquire a good data of scattering, a suitable concentration (5 × $10^{-3}$ mol $L^{-1}$) is chosen for the detection. As shown in Fig. 2c, the form factor derived from the plot of the scattering intensity (counts per area, $I$) and the scattering vector ($q$) is -2, suggesting a lamellar structure in the aqueous solution. Guinier fitting was carried out by plotting log ($Iq^2$) (y-axis) against $q^2$ (x-axis) (Fig. 2d). The lamellar thickness ($d$) can be figured out by the equation:

$$d = 2\sqrt{3}R_g \quad (1)$$

where $R_g$ is the gyration radius determined by the slop of the fitted line. Here, the thickness of TPE-11 aggregates is 6.3 ± 0.2 nm, which is comparable with the extended length of TPE-11 molecule. This result implies that the TPE-11 molecules should be parallel aligned in the aggregates, thus forming mono-molecule layered structures in the aqueous solution.

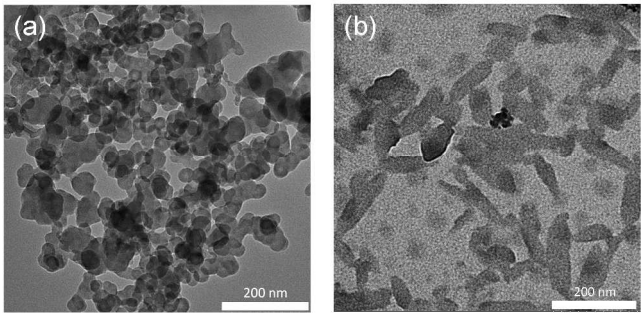


**Fig. 3** TEM images of the assemblies of TPE-11 at different concentrations: (a) 5 × $10^{-6}$ mol $L^{-1}$, (b) 1 × $10^{-3}$ mol $L^{-1}$.

In order to check if the self-assembled structures are stable during the dewetting process, TEM observation was carried out. In doing so, the solutions with certain concentration were casted on the copper net, and imaged without staining. As shown in Fig. 3, some flat nanostructures are obtained at the concentration of 5 × $10^{-6}$ mol $L^{-1}$, at which the nano-flakes are observed in the AFM image (Fig. 2a). Besides, the size of the flat structures shown by TEM is close to that shown by AFM, indicating that the nanostructures are stable against the drying process. In a similar way, we can conclude that the nanostructures formed at high concentration, taking 1 × $10^{-3}$ mol $L^{-1}$ for an example in Fig. 3b, is also stable.

Quantum yield ($\Phi$) is one of the characteristic parameters for the fluorogens. In order to test the fluorescent emission properties of the assemblies formed by TPE-11, $\Phi$ at different concentrations was measured using Rhodamine 6G as reference. The $\Phi$ of the sample can be calculated according to Equation 2, where $F$ is the fluorescence intensity, $\eta$ the refractive index of the solvent and $A$ the absorbance at the excitation wavelength.[64] The subscripts '$S$' and '$R$' are used to differentiate the sample and reference, respectively. When using the absorbance at the isosbestic point in the absorption spectra of the sample and the reference, $A_R$ equals to $A_S$ in value, and hence Equation 2 is abbreviated as Equation 3. Since $\Phi_R$ is known and equals to 0.95, $\Phi_S$ can be deduced by Equation 3, as long as $F_R$ and $F_S$ are measured. The $\Phi_S$s at different concentrations are plotted in Fig. 4a. Above the CMC, $\Phi$ increases with concentration, and reaches a plateau of 15% at around 1.6 × $10^{-5}$ mol $L^{-1}$, which is very close to the CTC of TPE-11.

$$\Phi_S = \frac{F_S}{F_R} \times \frac{(1-10^{-A_R})}{(1-10^{-A_S})} \times \frac{\eta_S^2}{\eta_R^2} \times \Phi_R \quad (2)$$

$$\Phi_S = \frac{F_S}{F_R} \times \frac{\eta_S^2}{\eta_R^2} \times \Phi_R \quad (3)$$

Meanwhile, the fluorescent emission properties are investigated by confocal laser scanning microscopy (CLSM). As shown in Fig. 4 b & c, in the concentration region of CMC - CTC and > CTC, where the flake-like and elongated flake-like nanostructures should be formed in the solution, bright dots and rods are observed, respectively. The shapes reflected by CLSM match well with the nanostructures formed in the solution.

In the following, the nano-fluorogens are used to label and map the cells. HeLa cell is selected as the target cell for test because of its remarkably durable and prolific property.[65] Before the measurement, the HeLa cells stored in liquid nitrogen were taken out, quickly thawed out, and cultured in RPMI-1640 medium supplemented with 10% fetal bovine serum (Hyclone) for 2 days. The cells were then split and seeded on the sterilized glass slides previously placed into the 6-well plate with cover glass. The density of seeding cells was about $10^4$ - $10^5$ per well. After 12 hours culture, the TPE-11 solution was added to the medium of adhesive HeLa cells on glass with concentration of 16 μg $mL^{-1}$ (1.3 × $10^{-5}$ mol $L^{-1}$), and continuously cultivated for 12 h, and observed by fluorescent microscope every one hour to check if the cells are stained with nano-fluorogens using 405 nm irradiating. When green fluorescent cells were observed, the medium with TPE-11 solution was changed by fresh RPMI-1640. Then the cells were washed with phosphate buffered saline twice, fixed with 4% polyformaldehyde for 15 min at room temperature. After fixation, the cells were washed with phosphate buffered saline twice to clear formaldehyde. The glass slides with adhesive cells were taken out, sealed and observed under confocal microscope.

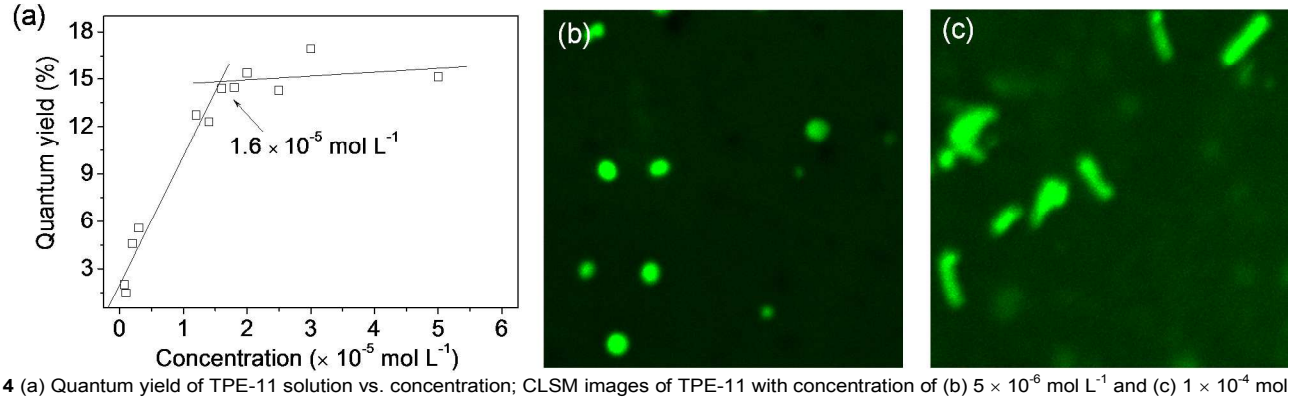


**Fig. 4** (a) Quantum yield of TPE-11 solution vs. concentration; CLSM images of TPE-11 with concentration of (b) $5 \times 10^{-6}$ mol $L^{-1}$ and (c) $1 \times 10^{-4}$ mol $L^{-1}$, excited by 405 nm laser.

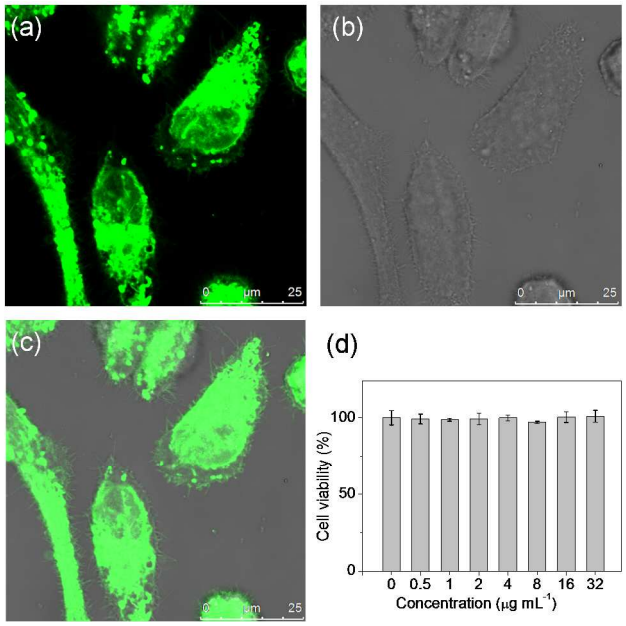


**Fig. 5** HeLa cells imaging with nano-fluorogens formed by TPE-11: (a) 405 nm excitations; (b) bright field; (c) merged images. (d) Biocompatibility test: dose-dependent cell viability of TPE-11 with HeLa cells.

Fig. 5a-c shows the CLSM images of HeLa cells with the excitation wavelength of 405 nm. The morphologies of the cells can be clearly discerned from the emission images of the nano-fluorogens formed by TPE-11. The fluorescent spots can be clearly seen in the cytoplasmic area of HeLa cells, and the intensity at nuclei region is relatively weak. This result indicates that the TPE-11 can readily penetrate into the HeLa cells, but not easily enter into the nuclei, which suggests that the nano-fluorogen has very strong interaction with cytoplasm, but weak attachment on the nuclei.

The biocompatibility of the nano-fluorogens formed by TPE-11 was evaluated by cell counting kit-8 (CCK8) assay (Dojindo, Japan). The preparation of the cells and incubation of nanofluorogens are similar to those in the cell imaging process. But here the concentration varied as 0.5, 1, 2, 4, 8, 16, 32 μg $mL^{-1}$. The dehydrogenases in cells were directly proportional to the number of living cells. The substrate WST-8 is reduced by dehydrogenases in cells to give a yellowish product---formazan, which is soluble in the cell culture medium. The measurements of formazan absorbance were carried out at 450 nm by micro-plate reader (multiskan mk3, Thermo Scientific, USA). The optical density values are proportional to the number of viable cells in the medium. As shown in Fig. 5d, the viabilities of HeLa cells were all above 98%, indicating an excellent biocompatibility of the nano-fluorogens formed by TPE-11.

## Experimental

### Materials and instruments

THF, petroleum ether, methanol, concentrated $H_2SO_4$, KOH, dichloromethane (DCM), ethyl acetate, HCl acid were purchased from Hangzhou Gaojing Fine Chemical Co., Ltd. 4-Bromo-benzoic acid, 3-methyl butynol, 11-bromo-1-undecanol, 4-dimethylaminopyridine (DMAP), dicyclohexylcarbodiimide (DCC), $Pd(PPh_3)_4$, CuI were bought from Sun Chemical Technology Co., Ltd, Shanghai. Triethylamine (TEA), $NaHCO_3$, anhydrous sodium carbonate, and 1-butanol were from Chinasun Specialty Products Co., Ltd. Diethyl ether was purchased from Hangzhou Chemical Reagent Co., Ltd.

$^1$H NMR spectra were recorded on a Bruker Advance 400 / 500 MHz. Liquid chromatography mass spectroscopy (LC-MS) analyses were performed on Aglient 1200/6220 with ESI resource produced by Agilent Technologies (USA). The fluorescence spectra were measured on Cary Eclypse Fluorescence Spectrometer manufactured by Varian Company, USA. The UV-vis spectra were recorded on Cary 60 spectrometer produced by Agilent Technologies (USA). The conductivities were measured with a digital conductivity instrument (DDS-307, Shanghai, P. R. China) at 25 °C.

The AFM images were taken on a multimode 8 microscope (Bruker, USA). Peak force QNM in fluid scan mode with ScanAsyst-Fluid$^+$ probe (nominal spring constants 0.7 N $m^{-1}$, frequency 120-180 kHz) purchased from Bruker was used during the in situ scanning. The data shown in the paper were processed with first order flatten and no more modification. SAXS (SAXSess mc2, Anton Paar GmbH, Austria) was used to get scattering data of aggregates in solution.

TEM was performed on Hitachi HT7700 (Japan) operating at 120 kV. 10 μL of the sample solution was placed onto a carbon-coated copper grid, and then the grid was dried in vacuum. The fluorescence images of the nano-fluorogens were taken on Leica TCS SP5 II (Germany).

In the cell imaging experiment, the sterilized glass slides were IWAKI PLL-coated cover glass, ASAHI Techno, Japan. Olympus fluorescent microscope (Japan) was employed to monitor the growth and labeling of the cells, and STP6000

confocal microscope (LEICA, Germany) was used to record the cell images.

**Synthesis of methyl 4-bromobenzoate (compound *A*)** 4-Bromobenzoic acid (5.0 g, 24.9 mmol) was dissolved in 150 mL methanol. Then concentrated sulfuric acid (6 mL) was added dropwise with stirring, and the mixture was refluxed for 12 h. After cooling down, the solvent was removed under reduced pressure. The residue was disolved in DCM, neutralized with saturated $NaHCO_3$ solution, and dried with rotavapor to get a white solid. Yield: 4.9 g, 91%. $\delta_H$ (500 MHz; $CDCl_3$; TMS): 7.91 (2H, d, $J$ = 8.5 Hz, Ar-H ortho to COO), 7.59 (2H, d, $J$ = 8.5 Hz, Ar-H meta to COO), 3.93 (3H, s, $COOCH_3$).

**Synthesis of methyl 4-(3-hydroxy-3-methylbut-1-yn-1-yl)benzoate (compound *B*)** Compound *A* (4.6 g, 20.0 mmol) and 2-methyl-3- butyne-2-ol (2.9 mL, 30.0 mmol) were added to a mixed solvent of anhydrous THF (100 mL) and TEA (6 mL). Meanwhile, $Pd(PPh_3)_2Cl_2$ (140 mg , 0.2 mmol) and CuI (40 mg, 0.2 mmol) were dissolved in the solution. After stirring for 1 h under argon atmosphere at room temperature, the mixture was refluxed for another 12 h. The resulting solution was neutralized with saturated $NaHCO_3$ solution, extracted with DCM, and purified by $SiO_2$ column chromatography to give a buff solid. Yield: 3.4 g, 79%.$\delta_H$ (400 MHz; DMSO-$d_6$; TMS): 7.94 (2H, d, $J$ = 8.4 Hz, Ar-H ortho to COO), 7.52 (2H, d, $J$ = 8.4 Hz, Ar-H meta to COO), 5.57 (1H, s, O*H*), 3.86 (3H, s, $COOCH_3$), 1.47 (6H, s, $C{\equiv}CC(CH_3)_2OH$).

**Synthesis of 4-ethynylbenzoic acid (compound *C*)** Compound *B* (4.0 g, 18.4 mmol) and KOH (10.2 g, 184.0 mmol) were dissolved in 60 mL butanol. The mixture was cooled down with ice bath after being refluxed for 10 min. The crude product, after filtration, was added to HCl acid solution with pH = 2, and then stirred for 2 h. The product was separated with extraction to get a yellow solid. Yield: 1.8 g, 68%. $\delta_H$ (400 MHz; DMSO-$d_6$; TMS): 13.12 (1H, s, COO*H*), 7.94 (2H, d, $J$ = 6.4 Hz, Ar-H ortho to COO), 7.60 (2H, d, $J$ = 6.4 Hz, Ar-H meta to COO), 4.46 (1H, s, *H*C≡C).

**Synthesis of 11-bromoundecyl 4-ethynylbenzoate (compound *D*)** Compound *C* (2.0 g, 13.7 mmol) and 11-bromo-1-undecanol (3.1 g, 12.4 mmol) were dissolved in 60 mL THF with DMAP (2 mg, 16.4 μmol). DCC (384 mg, 1.9 mmol, 15%) in 20 mL THF was added dropwise to the solution with ice bath and argon protection, and the reactants was stirred for 3 days at room temperature. The precipitate was filtrated, and the crude product was purified by $SiO_2$ column chromatography to give a white solid. Yield: 1.6 g, 31%. $\delta_H$ (400 MHz; DMSO-$d_6$; TMS): 7.92 (2H, d, $J$ = 6.8 Hz, Ar-H ortho to COO), 7.48 (2H, d, $J$ = 6.8 Hz, Ar-H meta to COO), 4.24 (2H, t, $J$ = 5.2 Hz, $CH_2OOC$), 3.33 (2H, t, $J$ = 5.2 Hz, $CH_2Br$), 3.17 (1H, s, *H*C≡C), 1.78 (2H, m, $CH_2CH_2OOC$), 1.69 (2H, m, $CH_2CH_2Br$), 1.37-1.21 (14H, m, $CH_2(CH_2)_7CH_2CH_2Br$).

**Synthesis of 1,2-bis(4-bromophenyl)-1,2-diphenylethene (compound *E*)** 4-Bromobenzophenone (500 mg, 1.9 mmol) and Zn (620 mg, 9.6 mmol) were added into morokuchi flask. Under nitrogen protection, 40 mL THF was add to the flask. Then $TiCl_4$ (0.3 mL, 2.6 mmol) was added at -78 °C, and kept stirring for 30 min. After being stirred at room temperature for 30 min, the reactant was refluxed for 7 h. The result product was extracted by DCM and then purified with $SiO_2$ column chromatography. Yield: 790 mg, 85%. $\delta_H$ (400 MHz; DMSO-$d_6$; TMS): 7.37-7.31 (4H, m), 7.18-7.11 (6H, m), 7.00-6.90 (8H, m).

**Synthesis of bis(11-bromoundecyl) 4,4'-(((1,2-diphenylethene-1,2-diyl)bis(4,1-phenylene))bis(ethyne-2,1-diyl))dibenzoate (compound *G*)** Compound *D* (622 mg, 1.6 mmol) and compound *E* (400 mg, 0.8 mmol) were added into 50 mL of THF, with existence of Pd (100 mg, 10%) and CuI (20 mg, 10%). Under the protection of argon, 5 mL TEA was added with stirring, and refluxed for 10 h. The resulting product was extracted with DCM and purified with $SiO_2$ column chromatography to give a yellow solid. Yield: 44 mg, 5%. $\delta_H$ (400 MHz; DMSO-$d_6$; TMS): 7.92 (4H, d, $J$ = 8.1 Hz, Ar-H ortho to COO), 7.46 (4H, q, Ar-H meta to COO), 7 .22 (4H, t, $J$ = 8.2 Hz, ), 7.07-7.04 (6H, m), 6.95 (8H, t, $J$ = 8.2 Hz), 4.24 (4H, t, $J$ = 6.5 Hz, $CH_2OOC$), 3.34 (4H, t, $J$ = 6.9 Hz, $CH_2Br$), 1.77 (4H, t, $J$ = 7.2 Hz, $CH_2CH_2OOC$), 1.68 (4H, t, $J$ = 6.9 Hz, $CH_2CH_2Br$), 1.18-1.36 (28H, m, $CH_2(CH_2)_7CH_2CH_2Br$).

**Synthesis of 1,1'-(((4,4'-(((1,2-diphenylethene-1,2-diyl)bis(4,1-phenylene))bis(ethyne-2,1-diyl))bis(benzoyl))bis(oxy))bis(undecane-11,1-diyl))bis(pyridin-1-ium) bromide (TPE-11)** Compound *G* (200 mg, 0.2 mmol) was added into 50 mL of pyridine and refluxed at for 2 days. After removing the solvent, the product was washed with ethyl ether for 5 times. Yield: 180 mg, 75%. $^1$H NMR spectrum is shown in Fig. S1 in the supporting information. $\delta_H$ (500 MHz; DMSO-$d_6$; TMS): 9.10 (4H, d, $J$ = 5.8 Hz, Ar-H ortho to $N^+$ ), 8.61 (2H, t, $J$ = 7.5 Hz, Ar-H para to $N^+$), 8.16 (4H, t, $J$ = 6.5 Hz, Ar-H meta to $N^+$), 7.97 (4H, t, $J$ = 6.4 Hz, Ar-H ortho to COO), 7.67 (4H, d, $J$ = 8.2 Hz, Ar-H meta to COO), 7.39 (4H, q, $J$ = 8.2 Hz), 7.22-7.17 (6H, m), 7.07-7.00 (8H, m), 4.59 (4H, t, $J$ = 7.3 Hz, $CH_2OOC$), 4.28 (4H, t, $J$ = 6.4 Hz, $CH_2Br$), 1.91 (4H, d, $J$ = 6.5 Hz, $CH_2CH_2OOC$), 1.71 (4H, t, $J$ = 6.6 Hz, $CH_2CH_2Br$), 1.39-1.26 (28H, m, $CH_2(CH_2)_7CH_2CH_2Br$); MS (ESI) *m/z*: $[M\text{-}2Br]^{2+}$ calcd: 542.305; found: 542.308.

## Conclusions

Through marriage the AIE effect and self-assembly of bolaamphiphiles, the mono-molecule layered nanostructures with good fluorescent emission properties have been achieved. It has been proven that the assemblies formed in the aqueous solution have two distinct mophologies depending on the concentration, and both are stable enough against the dewetting process. Due to the AIE effect, the self-assembled nanostructures emit strong green light and show quantum yield as high as 15%. More importantly, the nano-fluorogens can label HeLa cells without assist of any matrix and be successfully used to map the cell image by fluorescence. This work opens a novel avenue to fabricate water-soluble and biocompatible nano-fluorogens by self-assembly, and is anticipated to be extended to other AIE dyes and other bio-related detecting systems.

## Acknowledgements

The authors are in debt to Prof. L. Z. Fan and Mr. Z. T. Fan for helping us in contacting the cell imaging measurement. We would like to thank the National Natural Science Foundation of China (91127032, 21174035, 21274034, 21204054, 21233003), Excellent Young Teachers in Zhejiang Province and Hangzhou Normal University (HNUEYT 2011-01-019) for financial support.

## Notes and references

[a] Suzhou Key Laboratory of Macromolecular Design and Precision Synthesis, Jiangsu Key Laboratory of Advanced Functional Polymer Design and Application, College of Chemistry, Chemical Engineering

and Materials Science, Soochow University, Suzhou 215123, China. E-mail: songbo@suda.edu.cn
[b] College of Material Chemistry and Chemical Engineering, Hangzhou Normal University, Hangzhou 310036, China.
[c] Department of Cell Biology, School of Basic Medicine, Peking University Health Science Center, Beijing 100191, China.

† Electronic Supplementary Information (ESI) available: $^1$H NMR spectrum.

1 M. Zhang, L. Bai, W. Shang, W. Xie, H. Ma, Y. Fu, D. Fang, H. Sun, L. Fan, M. Han, C. Liu and S. Yang, *J. Mater. Chem.*, 2012, **22**, 7461.
2 D. Ding, K. Li, B. Liu and B. Z. Tang, *Acc. Chem. Res.*, 2013, **46**, 2441.
3 Y. Liu, Z. Wang, G. Zhang, W. Zhang, D. Zhang and X. Jiang, *Analyst*, 2012, **137**, 4654.
4 X. Wang, J. Hu, G. Zhang and S. Liu, *J. Am. Chem. Soc.*, 2014, **136**, 9890.
5 X. Shen, G. Zhang and D. Zhang, *Org. Lett.*, 2012, **14**, 1744.
6 X. Feng, L. Liu, S. Wang and D. Zhu, *Chem. Soc. Rev.*, 2010, **39**, 2411.
7 X. Mei, D. Chen, N. Li, Q. Xu, J. Ge, H. Li, B. Yang, Y. Xu and J. Lu, *Soft Matter*, 2012, **8**, 5309.
8 Y. Yu, C. Feng, Y. Hong, J. Liu, S. Chen, K. M. Ng, K. Q. Luo and B. Z. Tang, *Adv. Mater.*, 2011, **23**, 3298.
9 M. De, P. S. Ghosh and V. M. Rotello, *Adv. Mater.*, 2008, **20**, 4225.
10 Z. Zhelev, H. Ohba and R. Bakalova, *J. Am. Chem. Soc.*, 2006, **128**, 6324.
11 Y. Hong, J. W. Y. Lam and B. Z. Tang, *Chem. Soc. Rev.*, 2011, **40**, 5361.
12 R. Zhang, Y. Yuan, J. Liang, R. T. K. Kwok, Q. Zhu, G. Feng, J. Geng, B. Z. Tang and B. Liu, *ACS Appl. Mater. Interfaces*, 2014, **6**, 14302.
13 F. Wang, W. B. Tan, Y. Zhang, X. Fan and M. Wang, *Nanotechnology*, 2006, **17**, R1.
14 Y. G. Yanushevicha, D. B. Staroverova, A. P. Savitskyb, A. F. Fradkova, N. G. Gurskayaa, M. E. Bulinaa, K. A. Lukyanova and S. A. Lukyanova, *FEBS Letters*, 2002, **511**, 11.
15 Y. Su, M. Hu, C. Fan, Y. He, Q. Li, W. Li, L.-h. Wang, P. Shen and Q. Huang, *Biomaterials*, 2010, **31**, 4829.
16 Y. Hong, J. W. Y. Lam and B. Z. Tang, *Chem. Commun.*, 2009, 4332.
17 R. D. Moriarty, A. Martin, K. Adamson, E. O'Reilly, P. Mollard, R. J. Forster and T. E. Keyes, *Journal of Microscopy*, 2014, **253**, 204.
18 J. Luo, Z. Xie, J. W. Y. Lam, L. Cheng, H. Chen, C. Qiu, H. S. Kwok, X. Zhan, Y. Liu, D. Zhu and B. Z. Tang, *Chem. Commun.*, 2001, 1740.
19 Y. Dong, J. W. Y. Lam, A. Qin, J. Liu, Z. Li, B. Z. Tang, J. Sun and H. S. Kwok, *Appl. Phys. Lett.*, 2007, **91**, 011111.
20 A. Qin, C. K. W. Jim, Y. Tang, J. W. Y. Lam, J. Liu, F. Mahtab, P. Gao and B. Z. Tang, *J. Phys. Chem. B*, 2008, **112**, 9281.
21 S. Chen, J. Liu, Y. Liu, H. Su, Y. Hong, C. K. W. Jim, R. T. K. Kwok, N. Zhao, W. Qin, J. W. Y. Lam, K. S. Wong and B. Z. Tang, *Chem. Sci.*, 2012, **3**, 1804.
22 B.-K. An, S.-K. Kwon, S.-D. Jung and S. Y. Park, *J. Am. Chem. Soc.*, 2002, **124**, 14410.
23 C. J. Bhongale, C.-W. Chang, C.-S. Lee, E. W.-G. Diau and C.-S. Hsu, *J. Phys. Chem. B*, 2005, **109**, 13472.
24 M. Han and M. Hara, *J. Am. Chem. Soc.*, 2005, **127**, 10951.
25 Y. Qian, S. Li, G. Zhang, Q. Wang, S. Wang, H. Xu, C. Li, Y. Li and G. Yang, *J. Phys. Chem. B*, 2007, **111**, 5861.
26 Y.-T. Wu, M.-Y. Kuo, Y.-T. Chang, C.-C. Shin, T.-C. Wu, C.-C. Tai, T.-H. Cheng and W.-S. Liu, *Angew. Chem., Int. Ed.*, 2008, **47**, 9891.
27 C.-X. Yuan, X.-T. Tao, L. Wang, J.-X. Yang and M.-H. Jiang, *J. Phys. Chem. C*, 2009, **113**, 6809.
28 M. Wang, G. Zhang, D. Zhang, D. Zhu and B. Z. Tang, *J. Mater. Chem.*, 2010, **20**, 1858.
29 Y. Hong, L. Meng, S. Chen, C. W. T. Leung, L.-T. Da, M. Faisal, D.-A. Silva, J. Liu, J. W. Y. Lam, X. Huang and B. Z. Tang, *J. Am. Chem. Soc.*, 2011, **134**, 1680.
30 M. Faisal, Y. Hong, J. Liu, Y. Yu, J. W. Lam, A. Qin, P. Lu and B. Z. Tang, *Chemistry*, 2010, **16**, 4266.
31 D. Ding, K. Li, W. Qin, R. Zhan, Y. Hu, J. Liu, B. Z. Tang and B. Liu, *Advanced Healthcare Materials*, 2013, **2**, 500.
32 G. Wang, R. Zhang, C. Xu, R. Zhou, J. Dong, H. Bai and X. Zhan, *ACS Appl. Mater. Interfaces*, 2014, **6**, 11136.
33 Y. Hong, H. Xiong, J. W. Y. Lam, M. Häußler, J. Liu, Y. Yu, Y. Zhong, H. H. Y. Sung, I. D. Williams, K. S. Wong and B. Z. Tang, *Chem.-Eur. J.*, 2010, **16**, 1232.
34 F. Mahtab, Y. Yu, J. W. Y. Lam, J. Liu, B. Zhang, P. Lu, X. Zhang and B. Z. Tang, *Adv. Funct. Mater.*, 2011, **21**, 1733.
35 F. Mahtab, J. W. Lam, Y. Yu, J. Liu, W. Yuan, P. Lu and B. Z. Tang, *Small*, 2011, **7**, 1448.
36 X. Wu, S. Chang, X. Sun, Z. Guo, Y. Li, J. Tang, Y. Shen, J. Shi, H. Tian and W. Zhu, *Chem. Sci.*, 2013, **4**, 1221.
37 X. Zhang, X. Zhang, S. Wang, M. Liu, Y. Zhang, L. Tao and Y. Wei, *ACS Appl. Mater. Interfaces*, 2013, **5**, 1943.
38 H. Hachisako, N. Ryu and R. Murakami, *Org. Biomol. Chem.*, 2009, **7**, 2327.
39 H. Hachisako and R. Murakami, *Chem. Commun.*, 2006, 1073.
40 X. Zhang, X. Zhang, S. Wang, M. Liu, L. Tao and Y. Wei, *Nanoscale*, 2013, **5**, 147.
41 D. Yu, Q. Zhang, C. Wu, Y. Wang, L. Peng, D. Zhang, Z. Li and Y. Wang, *J. Phys. Chem. B*, 2010, **114**, 8934.
42 Q. Zhao, K. Li, S. Chen, A. Qin, D. Ding, S. Zhang, Y. Liu, B. Liu, J. Z. Sun and B. Z. Tang, *J. Mater. Chem.*, 2012, **22**, 15128.
43 C. Zhang, S. Jin, S. Li, X. Xue, J. Liu, Y. Huang, Y. Jiang, W.-Q. Chen, G. Zou and X.-J. Liang, *ACS Appl. Mater. Interfaces*, 2014, **6**, 5212.
44 H. Ringsdorf, B. Schlarb and J. Venzmer, *Angew. Chem., Int. Ed.*, 1988, **27**, 113.
45 M. Ahlers, W. Müller, A. Reichert, H. Ringsdorf and J. Venzmer, *Angew. Chem., Int. Ed.*, 1990, **29**, 1269.
46 T. Kunitake, *Angew. Chem., Int. Ed.*, 1992, **31**, 709.
47 J.-M. Lehn, *Chem. Soc. Rev.*, 2007, **36**, 151.
48 G. Wu, P. Verwilst, K. Liu, M. Smet, C. F. J. Faul and X. Zhang, *Chem. Sci.*, 2013, **4**, 4486.
49 B. Song, G. Liu, R. Xu, S. Yin, Z. Wang and X. Zhang, *Langmuir*, 2008, **24**, 3734.
50 S. Yin, C. Wang, B. Song, S. Chen and Z. Wang, *Langmuir*, 2009, **25**, 8968.



 

51 T. Kato, N. Mizoshita and K. Kishimoto, *Angew. Chem., Int. Ed.*, 2006, **45**, 38.
52 Y. Zhao, F. Sakai, L. Su, Y. Liu, K. Wei, G. Chen and M. Jiang, *Adv. Mater.*, 2013, **25**, 5215.
53 S. Wang, N. Zhang, X. Ge, Y. Wan, X. Li, L. Yan, Y. Xia and B. Song, *Soft Matter*, 2014, **10**, 4833.
54 Z. Wu, Y. Yan and J. Huang, *Langmuir*, 2014, 140610110300007.
55 L. Jiang, J. W. de Folter, J. Huang, A. P. Philipse, W. K. Kegel and A. V. Petukhov, *Angew. Chem., Int. Ed.*, 2013, **52**, 3364.
56 L. Xu, L. Jiang, M. Drechsler, Y. Sun, Z. Liu, J. Huang, B. Z. Tang, Z. Li, M. A. Cohen Stuart and Y. Yan, *J. Am. Chem. Soc.*, 2014, **136**, 1942.
57 H. Cao, X. Zhu and M. Liu, *Angew. Chem., Int. Ed.*, 2013, **52**, 4122.
58 P. Guo, P. Chen, W. Ma and M. Liu, *J. Mater. Chem.*, 2012, **22**, 20243.
59 G. Wu, J. Thomas, M. Smet, Z. Wang and X. Zhang, *Chem. Sci.*, 2014, **5**, 3267.
60 Y. Wang, P. Han, H. Xu, Z. Wang, X. Zhang and A. V. Kabanov, *Langmuir*, 2009, **26**, 709.
61 D. Yu, M. Deng, C. He, Y. Fan and Y. Wang, *Soft Matter*, 2011, **7**, 10773.
62 W. Z. Yuan, R. Hu, J. W. Lam, N. Xie, C. K. Jim and B. Z. Tang, *Chemistry*, 2012, **18**, 2847.
63 J. Huang, S. Wang, G. Wu, L. Yan, L. Dong, X. Lai, S. Yin and B. Song, *Soft Matter*, 2014, **10**, 1018.
64 Q. He, J. Shi, X. Cui, J. Zhao, Y. Chen and J. Zhou, *J. Mater. Chem.*, 2009, **19**, 3395.
65 R. Rahbari, T. Sheahan, V. Modes, P. Collier, C. Macfarlane and R. M. Badge, *Biotechniques*, 2009, **46**, 277.

Text:

Water-soluble nano-fluorogens are fabricated by self-assembly of a bolaamphiphile with AIE properties, and successfully applied in cell imaging.

Graphical abstract